Supporting Information for "Coupling of the subpolar gyre and the overturning circulation during abrupt glacial climate transitions"

M. Klockmann[1] *, U. Mikolajewicz[1], H. Kleppin[2], J. Marotzke[1]

[1]Max Planck Institute for Meteorology, Hamburg, Germany

[2]MARUM, Bremen, Germany

Contents of this file

1. Text S1 to S3
2. Figures S1 to S4

Corresponding author: M. Klockmann, Institute of Coastal Research, Helmholtz-Zentrum Geesthacht, Max-Planck-Str.1, 21502 Geesthacht, Germany (marlene.klockmann@hzg.de)

*Current affiliation: Institute of Coastal Research, Helmholtz-Zentrum Geesthacht, Geesthacht, Germany

Text S1: A Note on Defining the Subpolar Gyre We use the barotropic stream function to describe the subpolar gyre (SPG). The barotropic stream function is calculated by integrating the flow field over the entire water column. It thus includes the barotropic and the baroclinic flow. The dominant signal in the subpolar North Atlantic comes from the SPG circulation in the upper 500 m of the water column. Changes in the barotropic stream function can result from changes in either the barotropic or the baroclinic flow. Changes in the cross-gyre density difference (see Section 4 in the main manuscript) affect the baroclinic flow via the thermal wind relation.

Text S2: Complete and Incomplete Transitions We define the events with the respective strong AMOC phases centered at 2000, 3500, 5000, 6500 and 11500 simulation years as complete events. These events are also used to compute the composite AMOC response (see Fig. 1a in the main manuscript). Between simulation years 8000 and 10000, there is a kind of double event with two successive weaker AMOC peaks, which we have excluded from the composites. During these events, the density-driven feedback loop between the deep-water formation, the SPG state and the AMOC is absent. The efficient transport of salt from the subtropics to the subpolar regions does not set in and the transition to the strong AMOC state cannot be completed. The AMOC-SPG coupling during these incomplete transitions also differs from the coupling during the complete transitions because the density-driven feedback is missing (see also Fig. S1 and S2).

Text S3: Calculation of Implied Northward Salt Transport

The implied northward salt transport in Fig. 3f in the main manuscript and Fig. S2f is calculated from the freshwater budget of the Atlantic basin north of 40°N. The freshwater budget is defined as:

$$\frac{\partial}{\partial t} FWC_{Atl} = FWT_{Bering} + FWT_{40N} + netP_{Atl}, \tag{1}$$

where FWC_{Atl} is the freshwater content of the Atlantic north of 40°N, FWT_{Bering} the sum of the solid and liquid freshwater transport through Bering Strait, FWT_{40N} the ocean freshwater transport across 40°N and $netP_{Atl}$ the net precipitation (P-E+R) integrated over the Atlantic basin north of 40°N including the Arctic Ocean. The freshwater content and transport are calculated against a reference salinity, which is the simulated spatio-temporal average of the Atlantic salinity north of 40°N. The freshwater transport FWT_{40N} is then calculated as the residual from the change in freshwater content $\frac{\partial}{\partial t} FWC_{Atl}$, the transport through Bering Strait FWT_{Bering} and the net precipitation $netP_{Atl}$. This way, FWT_{40N} describes the sum of the diffusive and advective freshwater transport. Since a southward freshwater transport implies a northward salt transport, we express the implied northward salt transport as $(-1)xFWT_{40N}$.

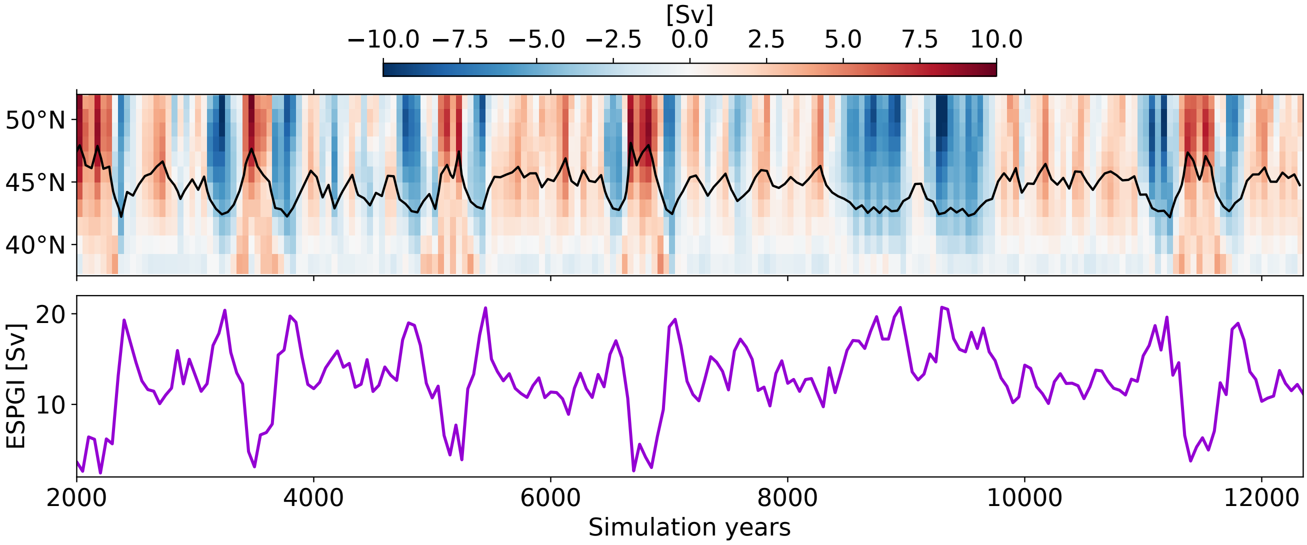

Figure S1. The anomaly described by the eastern subpolar gyre index (ESPGI) and its relation to the boundary between the SPG and the subtropical gyre. **(top)** Hovmoeller diagram of the anomaly of the barotropic stream function near 30°W (shading). The mean barotropic stream function was removed to obtain the anomalies. The black contour indicates the boundary between the two gyre. **(bottom)** The ESPGI as defined in the main manuscript. The ESPGI is closely related to the gyre boundary. When the ESPGI is high, the boundary is shifted southward; when the ESPGI is low, the boundary is shifted northward.

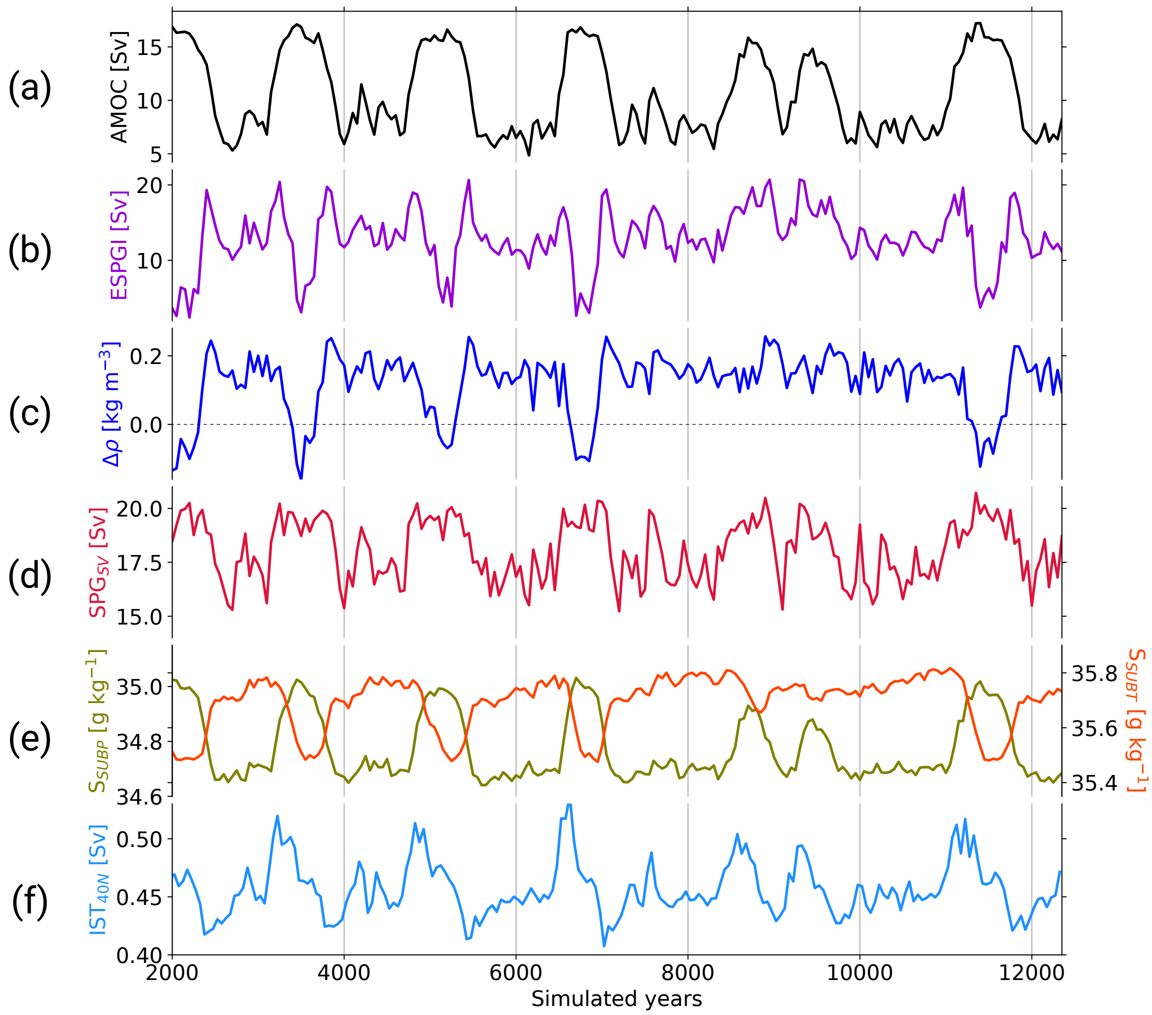

Figure S2. As Fig. 3 in the main manuscript but for the entire simulation. **(a)** maximum AMOC strength at 30°N; **(b)** eastern SPG index, calculated as the mean of the barotropic stream function in the red box in Fig. 2 in the main manuscript; **(c)** potential density difference averaged over the upper 500 m between the center and the rim of the SPG (see black boxes in Fig. 3g in the main manuscript). A positive difference indicates a higher density in the SPG center; **(d)** the maximum of the wind-driven SPG component obtained from the wind-stress curl via the Sverdrup relation; **(e)** salinity of the upper 1000 m in the subtropical (orange) and subpolar (olive) North Atlantic; **(f)** implied northward salt transport (IST) at 40°N, calculated from the freshwater budget of the North Atlantic as explained in the Text S2.

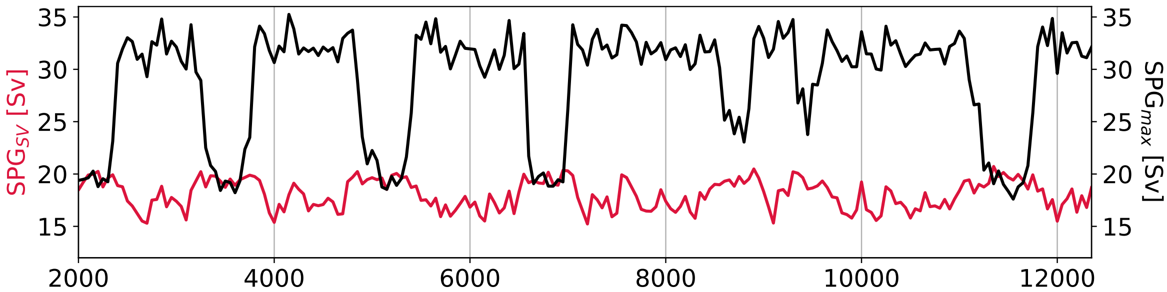

Figure S3. Timeseries of the wind-driven SPG transport, i.e. the maximum of the Sverdrup transport in the subpolar North Atlantic (red) and the total SPG transport, i.e. the maximum of the barotropic stream function in the subpolar North Atlantic (black). Both transports are multiplied by (-1).

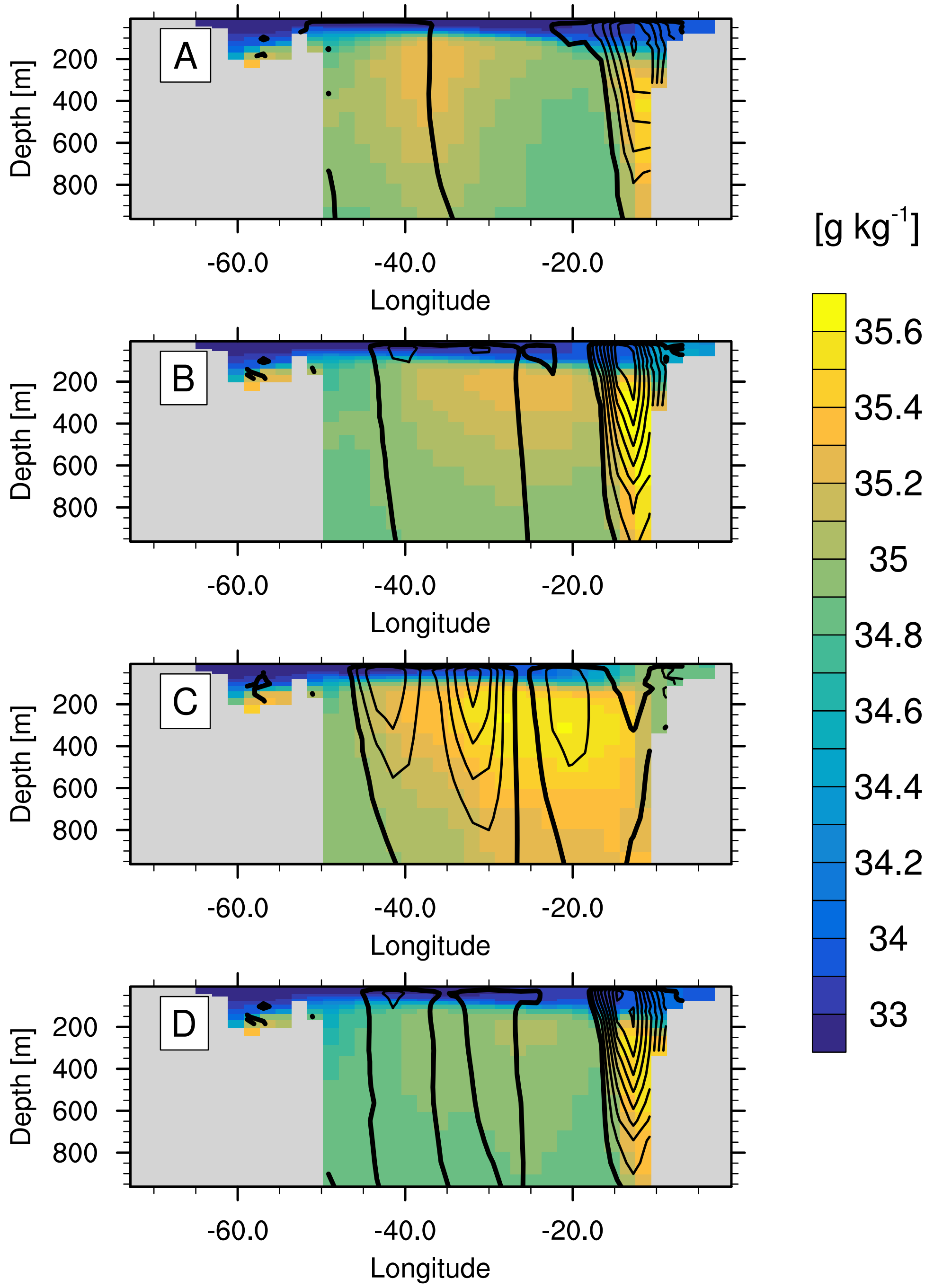

Figure S4. Transect of salinity (shading) and meridional velocity (contours) at the boundary between the subtropical and the subpolar gyre near 45°N. Only the northward velocity component perpendicular to the transect is shown. The bold contour indicates $0\,\mathrm{cm\,s^{-1}}$; the contour interval is $1\,\mathrm{cm\,s^{-1}}$. Shown are the 50-year means corresponding to the letters A,B,C and D in Fig. 2 and 3 in the main manuscript.